The morphological evolution of galaxy satellites

Lucio Mayer[1], Fabio Governato[2] and Monica Colpi[1]
[1]*Dipartimento di Fisica Universita' Degli Studi di Milano, Italy,* [2] *Osservatorio Astronomico di Brera, Merate, Italy*

Ben Moore[3], Thomas R. Quinn[4] and Carlton M. Baugh[3]
[3]*Physics Department, University of Durham, Science Labs., Durham, U.K,*
[4]*Department of Astronomy, University of Washington, Seattle, WA, USA*

Abstract.
We study the evolution of galaxy satellites with high resolution N-body simulations. Satellites are modeled as replicas of typical low and high surface brightness galaxies (LSBs and HSBs). Encounters on high eccentricity orbits (as typical in hierarchical models of galaxy formation) strip LSBs of most of their stars and tend to decrease their surface brightness. On the contrary, bar instability in HSBs leads to substantial loss of angular momentum of the stellar component and to an increase of central surface brightness. In both cases the remnant resembles a spheroidal galaxy with an exponential surface brightness profile. A simple modeling of color evolution and interactions driven star formation gives M/L ratios for the remnants that are roughly consistent with observations. These results suggest an evolutionary scenario for the dwarf galaxies in our Local Group, faint dSphs being the descendents of LSBs and brighter dSphs/dEs being the final state of HSB satellites.

1. Introduction

Our knowledge of the galaxies of the Local Group is becoming increasingly detailed: we have substantial information regarding star formation histories, kinematics and morphology of many faint dwarf satellites of the Milky Way and Andromeda (c.f. Mateo 1998 and references within).

The Local Group shows a morphology density relation that resembles that found in galaxy clusters (Dressler et al. 1998). Dwarf irregulars (dIrrs) are found mainly in the far reaches of the Local Group, while dwarf spheroidals (dSphs) and dwarf ellipticals (dSphs/dEs) are abundant close to the primary galaxies.

Detection of tidal streams in the halo of the Milky Way (de Zeeuw 1998) and peculiar structure of some of its closest neighbors (Ibata & Lewis 1998) suggest that mutual interactions between galaxies have played an important role in the evolution of all Local Group members.

In this contribution, we explore the effect that tidal interactions with the primary galaxies could have on accreting disk-like satellites.

2. Galaxy models

Galaxy models were built using the method developed by Hernquist (1993). We used observational constraints as well as theoretical models of galaxy formation (Cole et al. 1999) to make credible replicas of real galaxy satellites. Parameters for disk and halo components were chosen to represent typical HSB and LSB dwarf galaxies. We start by choosing a circular velocity ($V_c \sim 75$ km/s), comparable to that of large companions of spiral galaxies (Zaritsky et al. 1993), such as the LMC or NGC205 in our Local Group. The virial mass of the satellite is then determined by the circular velocity and is weakly dependent on cosmology (White & Frenk 1991) (we assumed a CDM model with $\Omega = 1$ and $h = 0.5$).

HSBs and LSBs obey the same B-band Tully Fisher relation on a large range of circular velocities (Zwaan et al. 1997): using this last relation we derive a value for the disk luminosity $L_B \sim 2 \times 10^9 L_\odot$. We assign the same disk mass to both HSBs and LSBs by assuming $M/L_B = 2$, as suggested by the generalized Bottema model (de Blok & McGaugh 1997). Disks are constructed using a Toomre parameter $Q = 2$, this being a necessary condition for global stability against bar modes (Friedli, these proceedings). The HSB disks have an exponential scale-length $r_h = 2$ kpc while we use $r_h = 5$ kpc for LSB disks: these values are consistent with the observed $V_c - r_h$ relation (Zwaan et al. 1997) and give a surface brightness $\mu_0 = 22$ mag arcsec^{-2} for the HSB satellite and $\mu_0 = 24$ mag arcsec^{-2} for the LSB satellite. This is in good agreement with average values found in the samples of de Blok & McGaugh (1997). Each galaxy model is embedded in an isothermal halo truncated at the virial radius (the same for both models as it depends only on V_c) : the halo is 60 times more massive than the disk and has a core radius r_c equal to r_h. Due to its larger core, the LSB model has a low-concentration halo and thus a slowly rising rotation curve, while the HSB satellite has a 3 times more concentrated halo and a steeply rising rotation curve, consistent with observations (de Blok & McGaugh 1997) (see Fig.1). M_{total}/M_{disk} at the "optical radius" $R_{opt} = 3r_h$ (see Persic and Salucci 1997) is equal to 4 for the HSB and is over 10 for the LSB satellite. We used about 200.000 particles for the halo and 50.000 particles for the disk of each satellite model.

Halo particles that pass through the disk are less massive (and hence proportionally more numerous) than halo particles whose orbits do not intersect the disk. This reduces disk heating due to two-body scattering by heavier halo particles (Lacey & Ostriker 1985, Velasquez & White 1998). The softenings are set to $0.06r_h$ for the disk, $0.4r_h$ for the lo-res halo particles and $0.35r_h$ for the hi-res ones. The models were evolved in

isolation for more than 5 Gyr to test their stability. At a fixed particle number we verified that disk heating is reduced by a factor of about 2 using a variable resolution model for the satellites' halos.

The primary galaxy is modeled as a Milky-Way sized isothermal halo ($V_c \sim 220$ km/s) truncated at the virial radius and whose mass is then 30 times larger than that of the satellites. It is represented by either a 50000 particles N-Body realization or simply by an external potential. This last configuration is preferable as it avoids numerical disk heating due to two-body scattering by massive particles belonging to the primary halo. Dynamical friction can be safely neglected because of the small mass of the satellites and the further delay resulting from tidal stripping (Colpi et al., in preparation). Our results are independent of the type of halo actually used.

3. Initial Conditions

We perform all of our simulations with the parallel treecode PKDGRAV (Stadel et al., in preparation) which has multistepping capabilities and uses local acceleration for the assignment of individual timesteps to particles. The minimum allowed timestep is $\sim 5 \times 10^5 yr$. Force calculations are done using a multipole expansion up to hexadecapole terms with a tolerance parameter $\theta = 0.7$. The satellite is put on a bound and very eccentric orbit (with $apo/peri = 10$ or 4) with an apocenter close to the virial radius of the primary system (consistent with the satellite just being accreted). Orbits of this kind are the most common for satellite halos in cosmological N-Body simulations (Ghigna et al. 1998). We run simulations with different relative orientations of the orbital angular momentum and spin of the satellite, from pure prograde encounters (vectors are parallel) to pure retrograde encounters (vectors are antiparallel). Several numerical tests (i.e varying timestep, tolerance and running identical i.c. with the TREECODEV3 by Barnes & Hernquist) were performed to ensure that results do not depend on the code or the particular choice of numerical parameters.

4. Results

HSBs and LSBs lose most of their dark matter halo after a few orbital periods (of typically 2 Gyr). The ratio M_{total}/M_{stars} at the initial R_{opt} has decreased to $1.5-4$ after $t \sim 7$ Gyr (see Fig.1). LSBs are structurally very fragile compared to HSBs: they end up with the smallest halos and lose up to 90% of their stellar mass, decreasing their total mass to
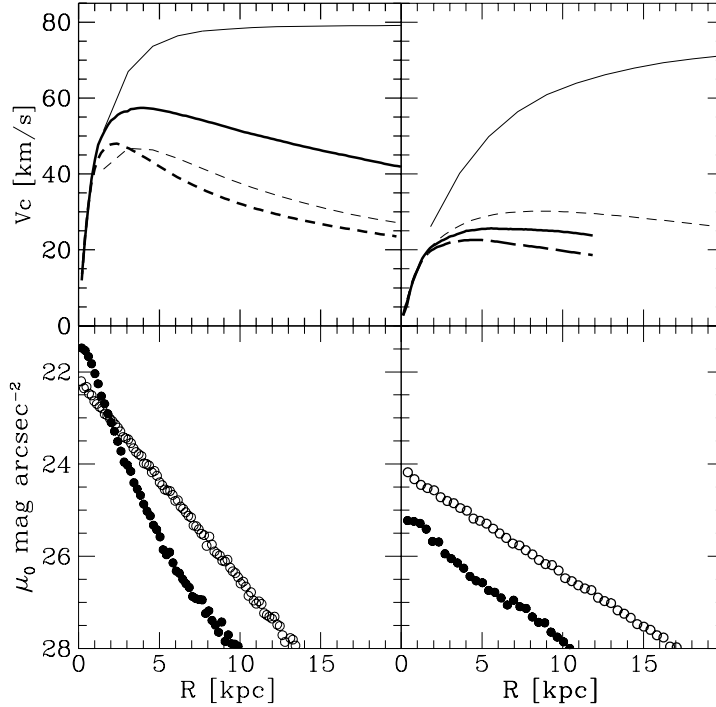
Figure 1. Left: HSB satellite on an orbit with *apo/peri* = 10. Right: LSB satellite on the same orbit. Upper panel: Evolution of circular velocity profiles ($V_c = \sqrt{(GM(r)/r)}$). Thin lines represent total profile (solid) and stellar profile (dashed) at $t = 0$. Thick lines represent total (solid) and stars (dashed) after $t \sim 7$ Gyr. Lower panels: Evolution of surface brightness profiles in the B band. Open dots are for $t = 0$, filled dots for $t \sim 7$ Gyr.

$\sim 10^8 M_\odot$. Instead, HSBs lose no more than 40% of their stellar mass and have final total masses in excess of $10^9 M_\odot$. The different response of the satellites is due primarily to the potential depth of the mass distribution and the disk scale-lengths (e.g. Moore 1999). A stellar bar appears after the first pericentric passage, its pattern being particularly strong for HSBs as a consequence of the higher disk surface density (Mihos et al. 1997). This leads to substantial angular momentum loss for HSBs disk particles (see Fig.2). The evolution of the satellites depends on the orbital parameters and disk/orbit orientation as well. Encounters on the more eccentric orbits are more damaging because the tidal field is stronger at small pericenters. Prograde encounters are a lot more destructive compared to retrograde ones (Toomre & Toomre 1972, Barnes 1988). Large tidal tails appear only in prograde encounters due to an approximate resonance between internal and orbital motions

(Springel & White 1998) and their extension is considerably larger in LSB galaxies because of their shallower halo density profile and larger disk scale-length (Fig. 2).

Stellar streams form which trace the orbital path of the satellite: their patterns are long lived. Tidal interactions have a profound influence on the morphology of the satellites, that evolve from disks to spheroids: the degree of flattening of the remnants varies from case to case, depending also on the disk/orbital plane orientation. The stellar remnants have final tidal radii in the range $6 - 10$ kpc. If we measure D_{25}, i.e. the radius containing a surface brightness higher than 25 mag arcsec^{-2}, the size of our remnants would never exceed $3 - 4$ kpc (see Fig.1). Remnants of LSBs could even be missed by some optical surveys. Remarkably, the projected density profile of the satellites steepens but remains close to exponential, with final scale lengths smaller than the initial ones. The central surface brightness increases by up to 1 mag arcsec^{-2} for HSBs due to the angular momentum loss, while it can decrease by about the same amount for LSBs on the most eccentric orbits (see Fig.1) The central dispersion behavior seems to follow that of the central surface density, increasing remarkably for HSB galaxies (coarse grained phase space density decreases, e.g. Hernquist et al. 1993). The final values are comparable with those observed in early-type dwarfs in our Local Group ($10 - 30$ km/s).

To derive mass-to-light ratios of the satellites to be compared with current observations, we have included a simple description of the evolution of the stellar component in an LSB satellite using stellar population synthesis models by Bruzual & Charlot (1993) with a Kennicutt IMF (Kennicutt 1994) and assuming a metallicity $Z \sim 1/3Z_{\odot}$, as typically inferred for LSBs (Gerritsen & de Blok 1999). We suppose the galaxy to form at $z \sim 2$ and enter the virial radius of the primary at $z \sim 1$, i.e. after 2 Gyr in our assumed cosmology.

Its star formation history is divided in three distinct phases: during the first 2 Gyr we assume an exponentially declining star formation rate (SFR) with a large time constant ($\tau = 10$ Gyr) and an amplitude of $0.2M_{\odot}/yr$, as suggested by observations and numerical simulations (Gerritsen & de Blok 1999). The satellite enters the primary with the mass and luminosity of our N-Body model. It then undergoes a central burst after the first pericentric passage (at $t \sim 4$ Gyr) as a consequence of bar formation and induced gas inflow (e.g. Lake et al. 1998). Finally we assume star formation to be truncated due to ram pressure and tidal stripping of gas, leading to passive evolution until the present time. The SFR during the burst has amplitudes going from 1 to $\sim 5M_{\odot}/yr$ and a duration of 50 Myr, as observed in blue star forming LSBs: a larger
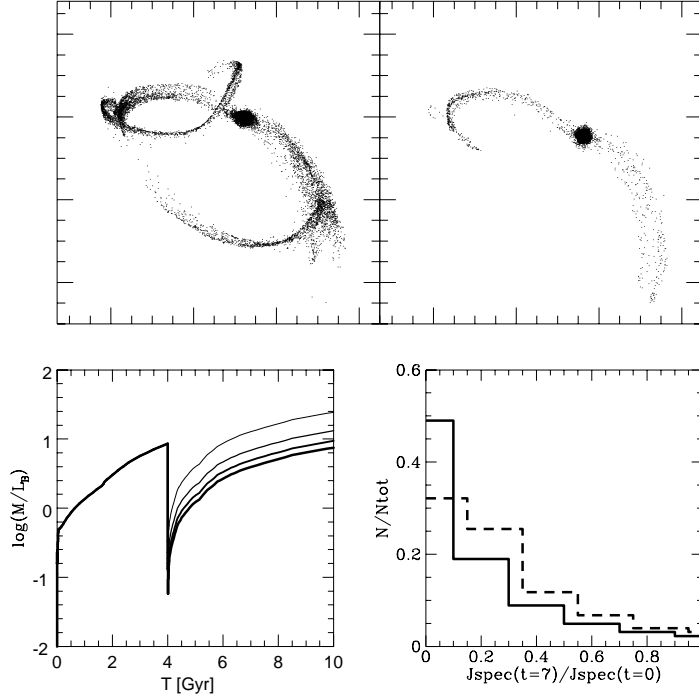
Figure 2. Upper left panel: disk particles of the LSB satellite after a coplanar prograde encounter, projected on the orbital plane. The box size is $390h^{-1}$ kpc. Upper right: same for the HSB model. Lower left panel: evolution of the M/L ratio (B band) for the LSB model assuming different burst strengths $(1, 2, 3, 5M_\odot/\text{yr})$, with thicker lines for stronger bursts. Lower right: distribution of final vs initial specific angular momentum for disk particles of LSB (dashed) and HSB (solid) satellites. Only particles that end up in the remnant are shown.

burst would be quite inconsistent with the low gas density and weak bar instability expected in an LSB galaxy.

At the present time the stellar mass-to-light ratio in the B band has a lower limit of ~ 7 (Fig. 2). A higher value, of the order of $11 - 12$, is obtained using solar metallicity or smaller bursts. However, dSphs have usually metallicity well less than solar (Grebel 1998).

Including the dark matter contribution, the final central mass-to-light ratio of our LSB satellites is at least $10-15$. However, mass-to-light ratios in dSphs are based on measures of the line-of-sight velocity dispersion, from which the central density is inferred. The remnants of LSBs have extended tails that can project along the line of sight: we find that we can overestimate the central dispersion by a factor of ~ 2 due to velocity gradients in the tails (Platek & Pryor 1995).

Thus, including also tidal effects we would measure central mass-to-light ratios in the range $10 - 40$ for the remnants of LSB satellites: similar values are found for many dSphs, like Leo I or Sagittarius A (Mateo 1998). Higher values (> 50) are necessary to match those of Draco and Ursa Minor. HSBs, on the contrary, are less affected by tides: the line-of-sight velocity dispersions are high at the end (~ 30 km/s) but reflect the velocity dispersion expected from virial equilibrium. Low total mass-to-light ratios (of the order of $2 - 6$) are inferred for dSphs/dEs like NGC205 (Mateo 1998). These are close to the values we obtain for M_{total}/M_{stars} in the remnants of HSBs. Thus, if we want these satellites to be ancestors of the brightest spheroidals, we need to suppose a more prolonged star formation to maintain low stellar mass-to-light ratios. Regions of recent star formation do exist in dSphs/dEs (Grebel 1998).

5. Conclusions

This work shows that *the long-lived interaction between a satellite and the primary galaxy can drive a dramatic morphological transformation between dwarf spirals to spheroidals.* After 2-3 pericenter passages LSB disk satellites resemble currently observed dSphs galaxies (see Mateo 1998). HSBs, instead, become more centrally concentrated and are likely the ancestors of more luminous dwarf ellipticals (dSphs/dEs). The increase in concentration is related to an interaction driven bar-instability which causes stars to lose substantial angular momentum.

The end products of interactions have lost plenty of dark matter during their evolution. Stars are no more a secondary mass component at the end, especially in the case of LSBs. However, a combination of fading of the stellar component and inflated velocity dispersions due to projection of tidal tails can produce M/L as high as those of many dSphs in the Local Group (Mateo 1998), while Draco and Ursa Minor need further investigation. A more prolonged star formation is requested to explain the observed M/L ratios of brighter dSphs/dEs.

It's tempting to associate our suggested picture for the evolution of galaxy satellites with the observed population of blue-compact galaxies at intermediate and high-redshift (Guzmán et al. 1997). We propose that those galaxies are disk-satellites undergoing morphological evolution and interaction induced star formation.

Moore et al. (1998, 1999) has shown that fast encounters between galaxies in clusters ("galaxy harassment") can drive their morphological evolution from disks to spheroids. This work shows that a similar scenario applies for large galaxy satellites, in a regime where the ratio

of relative/internal velocities is smaller. These results combine to show that tidal interactions provide a general, all purpose mechanism to evolve galaxies along the Hubble sequence. This is an alternative to the classic merger scenario and is likely to occur in a large variety of environments throughout the history of the Universe.

References

Barnes J.E. 1988, *Ap.J.*, **331**, 699

Bruzual G. & Charlot S. 1993, *Ap.J.* **405**, 538

Cole S., Lacey C. G., Baugh C. M. & Frenk C. 1999, in preparation

Colpi M., Mayer L., Governato F. & Quinn, T. 1999, in preparation

de Blok W.J.G. & McGaugh S.S. 1997, *M.N.R.A.S.*, 290,533

Dressler A., Oemler, A., Couch, W.J., Smail I., Ellis R.S, Barger A., Butcher H., Poggianti B.M., Sharples R.M. 1998 *Ap.J.* **409**, 577

Ghigna S., Moore B., Governato F., Lake G., Quinn T. & Stadel J. 1998, *M.N.R.A.S*, **299**, 515

Gerritsen J.P.E. & de Blok W.J.G. 1999 , *A & A*, **342**, 655

Grebel E.K., 1998, *astro-ph/9806191*

Guzmán R., Gallego J., Koo D.C., Phillips A.C., Lowenthal J.D., Faber S.M., Illingworth G.D., Vogt N.P. 1997, *Ap.J.*, **489**, 559

Hernquist L. 1993, *Ap.J.Suppl.*, **86**, 389

Hernquist L. Spergel D.N. Heyl J.S. 1993, *Ap.J.*, **416**,415

Ibata R.A. & Lewis, G.F. 1998, *Ap.J.*, **500**, 575

Kennicutt R.C. & Tamblyn P. 1994, *Ap.J.*, **435**, 22

Lacey C. & Ostriker J.P. 1985, *Ap.J.*, **176**, 1

Lake G., Katz N. & Moore, B. 1998, *Ap.J.*, **495**, 152

Mateo M. 1998, *astro-ph/98100070*

Mihos J.C., McCaugh S.S. & De Blok W.J.G. 1997, *ApJL*, **477**,L79

Moore B., Katz N., Lake G., Dressler A. & Oemler A. 1996, *Nature*, **379**, 613

Moore B., Lake G. & Katz N. 1998, *Ap.J.*, **435**, 139

Moore B., Lake G. , Quinn T. & Stadel J. 1999, *MNRAS*, in press

Persic M. & Salucci P. 1997, *Dark and visible matter in galaxies ASP ConferenceSeries*, 117 ed. M.Persic P.Salucci

Platek, S. & Pryor, S. 1995, *Astron. Journal*, **109**, 1071

Springel V. & White S.D.M. 1998, *astro-ph/9807320*

Velazquez H. & White S.D.M. 1998,*astro-ph/9809412*

Toomre & Toomre 1972, *Ap.J.*, 178, 623

Zaritsky D., Smith R., Frenk C. & White S.D.M. 1993, *Ap.J.*, **405**, 464

Zwaan M.A., Van der Hulst J.M., de Blok W.J.G. & Mc Gaugh S.S. 1995, *M.N.R.A.S.*, **273**, L35